

Diagnosis of Neurodegenerative Disorders in Brain MRI Using Tissue Variation and SVM Classifier

N.Ahanapriyanka and G.Kavitha'

Department of Electronics Engineering, MIT Campus, Anna University, Chennai, ahanachellian@gmail.com

Abstract—Dementia is a neurological impairment, which results in loss of mental ability to perform a regular task. Alzheimer disease (AD) and Mild Cognitive impairment (MCI) are most common forms of dementia. The tissue variation in brain helps to identify the pathological changes in these disease progressions. Thus, an attempt is made to diagnose the severity of such neurodegenerative disorders based on pattern changes in brain tissues. Initially, MR images are pre-processed using robust brain extraction (ROBEX) tool. The skull stripped images are subjected to Tsallis entropy based on multilevel thresholding to segment the brain tissues such as white matter (WM), gray matter (GM) and cerebrospinal fluid (CSF). Pyramid histogram of gradient (PHOG) and Zernike moments (ZM) features are extracted from different segmented brain tissues for normal, MCI and AD. The significant features selected based on principal component analysis (PCA) are subjected to least square SVM (LSSVM) and SVM classifiers. Result shows that prominent tissue variations are observed in PHOG features compared with ZM. It is noticed that SVM classifier is able to classify the normal, MCI and AD images better than LSSVM. Higher classification accuracy is obtained for GM. These finding suggest that GM is able to show significant difference between normal, MCI and AD subjects. Thus, this study could aid to analyse the brain tissue interior variation and connection between neurodegenerative disorders. Hence this approach could be used as a supplement in the investigation of dementia disorder.

Keywords—Alzheimer disease, mild cognitive impairment, brain tissue, white matter, gray matter, cerebrospinal fluid, pyramids histogram of gradient(PHOG), Zernike moment(ZM)

I. INTRODUCTION

Dementia is the most common chronic degenerative symptom. This leads to various brain disorders such as Alzheimer (AD), Mild cognitive impairment (MCI), Vascular Dementia, Dementia with Lewy Bodies (DLB), Frontotemporal Dementia (FTD) and mixed dementia. AD and MCI is recognized as important cognitive problem as a dementia risk [1]. Various researches suggest that subjects with MCI have greater chance to convert into AD due to prominent memory disturbance. Approximately 50 million people worldwide live with dementia [2]. It causes major impact in cognitive skill and cause difficulty to lead a social economic life. The identification of cognitive feature is of greater importance to provide an advent treatment. Currently, diagnosis of dementia relies on clinical assessment which limits to highlight the substantial changes in the brain regions. However, many studies suggest that tissue variations of these disorders incorporate the potential information about the diseases progression [3].

The diagnostic strategy for these degenerative disorders can be developed with the combination of clinical assessment and analysis of pathological changes [4]. These changes are generally observed by Magnetic Resonance (MR) imaging. It is a noninvasive, nondestructive and flexible imaging technique that does not require ionizing radiation.

The MR brain images relatively contain extra-cranial tissue. The delineation of these extra-cranial tissues requires preprocessing which is commonly referred as skull stripping. Various techniques [5] such as morphological operation, elastic registration and tissue segmentation are used to separate the brain from extra-cranial tissues. Based on various report Robust learning based Brain Extraction System (ROBEX) tool results better delineation of T1 weighted MR brain image [6]. It is based on point distribution model adjusted by using voxel classification with random forest algorithm. This helps to identify discrimination in tissue effectively.

Recently, a variety of data analysis and machine learning methods are used to discriminate among normal, MCI and AD subjects. Based on various study deterioration of brain widely affect the brain tissue regions such as White matter (WM), Gray matter (GM) and cerebrospinal fluid (CSF) [7]. Diagnosis of tissue variation in these disorders is challenging due to heterogeneous pattern that is analogous to other brain disorder. A precise and accurate diagnosis of these tissues variation would facilitate the diagnosis and understanding of this disease. Hence, segmentation is carried out.

Segmentation of brain tissue is a tough task due to the irregular intensity between tissues and its boundaries [8]. Many techniques such as voxel based method, vertex based method, thresholding, clustering, graph based method and Region of Interest (ROI) have been attempted for segmentation of brain tissues [9]. Among them thresholding is commonly used. In an image, pixel with gray level values higher than a certain threshold value 'T' are categorized as object of the image and remaining gray level values are lesser than 'T' are categorized as background image [10]. However, in case of medical image, bi-level thresholding does not give appropriate performance. As a result, there is strong requirement for multilevel thresholding. Tsallis entropy is simple to implement and easily extended to multilevel thresholding problems compared to other entropy due to its non extensive property [11]. The moment-preserving principle used to select the thresholds of the gray-level image. The segmentation result requires quantification study to understand its pathology. Hence quantification is carried out by feature extraction techniques.

Now-a-days, feature based analyses are utilized in the study of complicated disorders associated to brain of human for the reliable diagnosis. Zernike moment (ZM) [12] and Pyramid Histogram of gradient (PHOG) [13] descriptors are considered for this study. These features have been effectively used in variety of medical image analysis including detection of tumors and degenerative disorders. However, identifying discriminative features is challenging owing to the large set feature.

Feature selection method help to identify the prominent feature set. In this study, feature selection is performed using principal component analysis (PCA). This method effectively represents the intrinsic pattern of the given features [14]. This methodology has been applied to face recognition and image denoising techniques. Neuroanatomical pattern classification has recently facilitated the identification of imaging biomarkers. Recently various machine learning techniques are applied for classification. Among them, SVM [15] and least square SVM (LS-SVM) [16] classifier is widely used in EEG signal classification, schizophrenia, breast cancer and breast microscopic images. Hence in this work SVM and LS-SVM are adopted for classification of normal, MCI and AD images.

The contribution of this work is to identify the variations of normal, MCI and AD subjects in their neuroanatomical region of brain MR images. This study precisely made to interpret the

tissue pattern changes in WM, GM and CSF effectively. Initially T1 weighted MR brain images are skull stripped using ROBEX tool. Then the images are subjected to segmentation using multilevel Tsallis entropy based segmentation for delineation of brain tissue. Different features such as ZM and PHOG are extracted from segmented brain tissue. Then, the effective feature set is identified using PCA. These feature sets are help to discriminate and analyse the tissue pattern changes. Finally, SVM and LS-SVM is used to classify normal, MCI and AD images.

The paper is structured as follows. In Section 2 brief description of methods that includes dataset details, skull-stripping, feature extraction, feature selection and classifier are focused. Section 3 presents the results and discussions of framework. Finally, the conclusions are given in Section 4.

II. METHODS AND MATERIALS

The flow diagram of the work is depicted in Fig. 1. The input images, obtained from publically available database are exposed to skull-stripping process using ROBEX tool. Segmentation of various brain tissues are carried out using multilevel Tsallis entropy. The pattern variations features such as ZM and PHOG are extracted from segmented brain tissue. The significant features are selected using PCA, and are classified as normal, MCI and AD using SVM and LS-SVM classifiers.

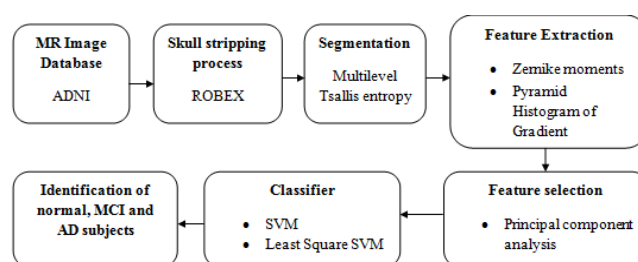


Fig. 1. Flow diagram of the proposed work

IMAGE DATABASE

In this study, total of 750 images (N=250, MCI=250 and AD=250) are considered. The images are acquired from Alzheimer's Disease Neuroimaging Initiative (ADNI) database (<http://adni.loni.usc.edu/data-samples/>). The T1-weighted transaxial view MR images are used for the analysis. The MCI and AD images are selected based on the Mini mental state examination (MMSE) and clinical dementia rating (CDR) score which is available in the database. All the MR scans are atlas registered and bias field corrected images. These MR images are subjected to further processing.

SKULL STRIPPING

The normal, MCI and AD T1 weighted MR Images are skull stripped using ROBEX tool. It is based on the combination of generative and discriminative model to delineate the non brain

tissue [6]. The brain boundary is detected with the help of discriminative model using random forest classifier. The generative model finds the contour of brain tissue with highest like hood in accordance with discriminative model. The contours are obtained using graph cut method to attain the target shape. Thus the tool produces the result with improved intensity standardization, higher boundary probability volume and better final segmentation.

MULTILEVEL TSALLIS ENTROPY BASED SEGMENTATION

Multilevel thresholding uses more than one threshold value and creates an output image with multiple groups [17]. Tsallis entropy is used to measure the improbability of the system. Tsallis entropy can be extended to non-extensive system based on a general entropic formula which is represented in Eq. (1) [18].

$$s_q = \frac{1 - \sum_{i=1}^k (p_i)^q}{q-1} \quad (1)$$

where k is the total number of possibilities of the system and q is the measure of degree of non-extensivity of the system called Tsallis parameter or entropic index . This entropic form can be extended for a statistical independent system by a pseudo-additive entropic rule which is expressed in Eq. (2) [11].

$$s_q^{A+B}(t) = s_q^A(t) + s_q^B(t) + (1-q)s_q^A(t)s_q^B(t) \quad (2)$$

This method is used to obtain threshold value for segmentation of an image. The information measure between required classes is maximized and the corresponding gray level is considered to be the desired threshold values of particular region. Tsallis entropy of an image I depends on the desired threshold t. Here, $s_q^A(t)$ and $s_q^B(t)$ represent the entropy of each class, and the third term $s_q^A(t)s_q^B(t)$ represents the interaction between the threshold classes. Parameter q can be lesser or greater than 1. The value of q is less than one as the entropy becomes sub-extensive and greater than one as the entropy become super-extensive. In this work, non-extensiveness parameter 'q' is considered to be 0.5 in order to improve the correlation and effectiveness of the threshold values.

ZERNIKE MOMENT (ZM)

ZM is a global descriptor with the class of orthogonal moments. ZMs belong to the class of orthogonal rotation invariant moments (ORIMs). It is obtained by projecting the input image onto the complex orthogonal Zernike polynomials. The discrete form of the ZM for an image with the size $N \times N$ is expressed as follows [12],

$$z_{n,m} = \frac{n+1}{\lambda_N} \sum_{C=0}^{N-1} \sum_{r=0}^{N-1} f(x,y) V_{n,m}(x,y) \quad \text{Where} \quad (3)$$

$$V_{n,m}(x,y) = R_{n,m}(\rho_{xy}) e^{-jm\theta_{xy}}$$

In Eq. (3) $V_{n,m}(x,y)$ is the Zernike basis functions, $R_{n,m}$ is a radial polynomial and ρ is the length of vector from the origin to (x, y) with the range of $0 \leq xy \leq 1$, where N is a normalization factor. This enables the contribution of each moment to be unique and independent of information in an image. To analyze the performance and effectiveness of ZM a group of high-order and low-order moments have been extracted from normal, MCI and AD images. The first, second and third group includes 36, 44 and 25 moments which is based on Eq. (4).

$$Group1 = \begin{cases} 1 \leq n \leq 10 \\ |m| \leq n \\ n - |m| = 2k \\ k \in N \end{cases} \text{ and } Group2 \ \& \ 3 = \begin{cases} 11 \leq n \leq 20 \\ |m| \leq n \\ n - |m| = 4k \text{ for} \\ \text{group2} \\ n - |m| = 8k \text{ for} \\ \text{group3} \\ k \in N \end{cases} \quad (4)$$

PYRAMID HISTOGRAM OF GRADIENT (PHOG)

PHOG descriptors are used to represent the shape and spatial patterns of an image. The objective of the PHOG [19] is to take the spatial property of the local variation into account. In PHOG edge contours are extracted using the Canny edge detector for an image. The grid at resolution level (L) had desires cells along each dimension. The orientation gradients are then computed using a 3*3 Sobel mask without Gaussian smoothing [20]. Here shape descriptors are used in the orientation range [0-180]. PHOG bin size is fixed throughout as k bins (here k = 8). Each PHOG feature for the entire image is a vector with the dimensionality $k \sum_{l=L} 4^l$.

Finally, based on the levels L, the images are divided and HOG is computed. Finally, the histograms of all the blocks consist of a whole HOG descriptor.

PRINICIPAL COMPONENT ANALYSIS (PCA)

PCA is able to transform samples into a new space and to use lower-dimensional representation from the new space to denote the sample. Consider m be the numbers of features are taken, with respect to n as $m \times n$ matrix A. Let $k < n$ be the dimensionality of the space that seeks to embed features. Assume that the columns (features) of A are mean-centered [21]. Then, PCA returns the top k left singular vectors of A as $m \times k$ matrix P_k . After that projects the data on the k-dimensional subspace spanned by the columns of P_k . Let $M_{U_k} = U_k U_k^T$ be the projector matrix on the resultant subspace. It is well-known that the resulting projection is optimal in its residual which is represent in Eq. (5),

$$\|A - P_{U_k} A\| \xi \quad (5)$$

Thus this process minimized over all possible k-dimensional subspaces.

CLASSIFIER

Support vector machine (SVM) maps the input points into a high-dimensional feature space and finds a separating hyperplane that maximizes the margin between two classes in this space. Without any knowledge of the mapping, the SVM finds the optimal hyperplane by using the dot product functions in feature space that are called kernels [22]. The solution of the optimal hyperplane can be written as a combination of a few input points that are called support vectors. In the feature space, the decision function that separates classes is given as Eq. (6)

$$D(x) = w^T \phi(x) + b \quad (6)$$

Where w and b is the one dimensional vector and bias term respectively. Then the SVM is formulated in the primal form as,

$$Q = \frac{1}{2} w^T w + c \sum_{i=1}^M \xi_i \text{ subject to } y_i D(x_i) \geq 1 - \xi_i \quad (7)$$

In Eq. (7), ξ_i are artificial slack variables representing classifier errors and C is a constant. It used to avoid parameter sensitivity.

The Least Square SVM is the Least Square interpretation of Support Vector Machine. It finds the pattern in the data which can be used for classification and regression analysis [23]. This approach minimizes the sum of squares of the errors made in the results of every single equation to determine the line of best fit to the model. In LS-SVM for function estimation, the optimization problem is formulated as [24]

$$\min_{a,b,c} J(a, e) = \frac{1}{2} \|a\|^2 + \frac{1}{2} \gamma \sum_{k=1}^N e_k^2 \quad (8)$$

Where, $e_k \in \mathbb{R}$ are error variables; and $\gamma \geq 0$ is regularization constant. To solve this optimization problem, Lagrange function is constructed as

$$\frac{1}{2} \|a\|^2 + \frac{1}{2} \gamma \sum_{k=1}^N e_k^2 - \sum_{k=1}^N \alpha_k \{ e_k + (w, \phi(x_k)) + b - y_k \} \quad (9)$$

where, $\alpha_k \in \mathbb{R}$ are Lagrange multipliers. Solving by differentiating the above Eq. (8) and Eq. (9) least square model can be solved in kernel space. This will improve the robustness of the classifier.

III. RESULT AND DISCUSSION

The image dataset used in this work includes normal, MCI and AD subjects. The MR brain images are skull stripped using ROBEX tools. The T1 weighted axial view of MR images are skull stripped. Fig.2 (a) shows the original image in the database. The corresponding skull stripped images are shown in Fig. 2(b). Visual results show that the ROBEX tool is able to extract the whole brain tissues better for both normal, MCI and AD subjects. It is able to observed the there exist a tissue variation in delineated images as the disease progresses. Finally, the obtained skull strip images are used for segmentation. This automated skull stripping methods help to improve the accuracy of prognostic and diagnostic procedures in brain image segmentation and analysis.

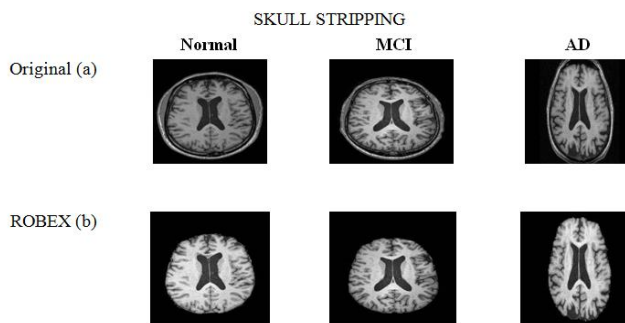


Fig. 2. Skull Stripping using ROBEX (a) Typical MR image and (b) Segmented Whole brain image

Fig. 3(a) represents T1 weighted MR image of Normal, MCI and AD subjects. Fig. 3 (b), (c), (d) and (e) represent the segmented image, white matter, grey matter and CSF. The visual representation of the images indicates there exist the tissue variation among normal, MCI and

AD subjects respectively. In the Fig 3(a) original image, it is evident the visibility of different tissues is strongly dependent on the different threshold values.

In Segmentation Tsallis entropy is used to segment the tissue. Based on global and objective property of the image histogram in Tsallis entropy it is suitable to implement in multilevel thresholding case. Parameters are tuned for Tsallis to improve the image thresholding values to segment the brain tissue. It is observed from segmented image in Fig.3 (b) that brighter, darker and background regions are well separated by different threshold values to obtain different tissues.

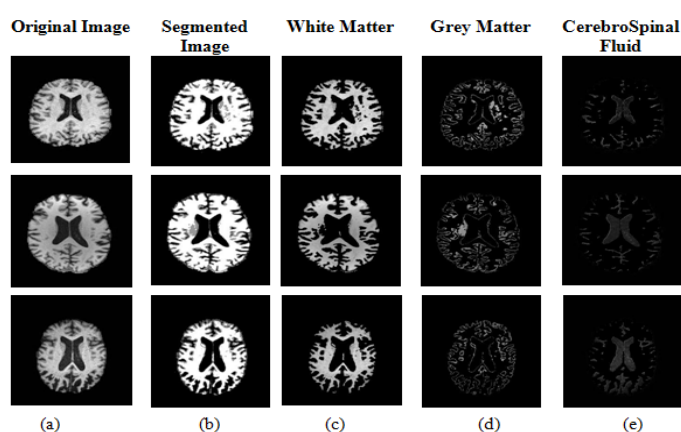


Fig. 3. Segmentation of Brian Tissue (a) Typical MR image (b) Segmented image (c) White matter (d) Grey matter (e) Cerebrospinal fluid (1st, 2nd and 3rd row represent the normal, MCI and AD respectively)

Then from the segmented WM, GM and CSF- PHOG and ZM features are extracted for normal, MCI and AD images. PHOG features is extracted for L=1, 2, 3 levels which indicate the number of pyramids. Fig. 4 (a), (b) and (c) depicts PHOG descriptor at each level respectively.

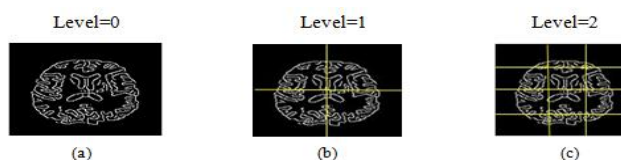


Fig. 4. Typical Representation of PHOG feature at each level (a) Level=0 (b) Level=1 and (c) Level=2

From the Table I. It shows each level corresponding to different set of features.

TABLE I. FEATURES EXTRACTED FROM THE SEGMENTED IMAGE

Pyramid Histogram of Gradient		
Level	Bin	Number of Features
1	8	40
2	8	168
3	8	680
Zernike moment		
Group	order (n)	Number of moments
1	1-10	36
2	11-20	44
3	11-20	25

Zernike moment is based on orthogonal property where moment represents the descriptor information of an image. Zernike feature require moment order (n) and repetition moments (m) to extract the features. Here Zernike amplitude features for three groups such as (G=1, 2, 3) are extracted. To analyze the effect of orders of Zernike moments on the performance of the

overall system, a group of high-order and low-order Zernike moments have been extracted. These three groups of Zernike moments are analysed to determine the various detail of the tissue.

The extracted features from PHOG and ZM for different order and various levels are given to feature selection method. PCA perform selection based on the highest eigen values. The obtain eigen value is used to select the significant features set.

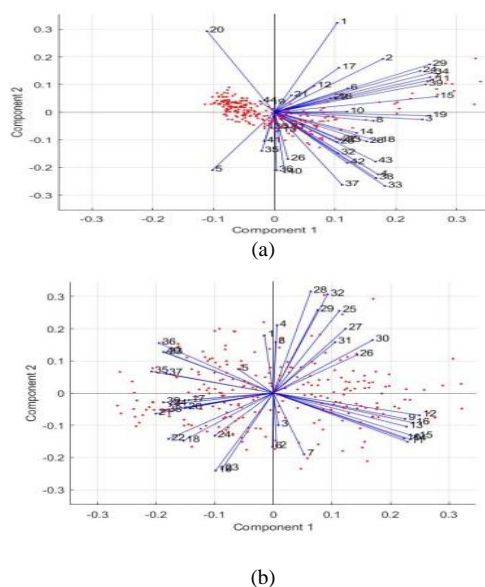


Fig. 5. Biplot representation of (a) Zernike moments and (b) PHOG features

The multivariate features of PCA can be visually represents by means of biplot. In biplot the features in original space are more representatives in the new generated space. In Fig. 5, PCA biplots allow visualization of the magnitude and sign of each features contribution to the largest two principal components. The x-axis is represented by principal component 1 and the y-axis by Principal component 2. In the above biplots, PCA scores are represented in red points and the original features are represented in blue vectors. The distance between the scores and the vector shows how much the score influences the vector or vice versa [25]. If the score are situated on the opposite side of the PC coordinate compared to the vector then the scores have less effect on features. This factor determines the influence of significant features. The size of the angle between vectors determines the correlation of the features. A longer vector means the variable is well represented by the plot and vice versa. A small angle indicates a strong positive correlation, 90 degrees represents no correlation and 180 degrees represents a negative correlation.

A visual analysis of the biplots indicates that Zernike and PHOG methods seem to capture the information in different ways, as evidenced both by the different nature of the radial dependence of features with respect to the first two principal components as well as by the respective distribution of the scores. In ZM feature the score are less influence to the vector when compare to PHOG. The angle of projection for PHOG and ZM comparison of actual vector lengths in the biplots is difficult, largely due to the matrix-specific PCA variable scaling.

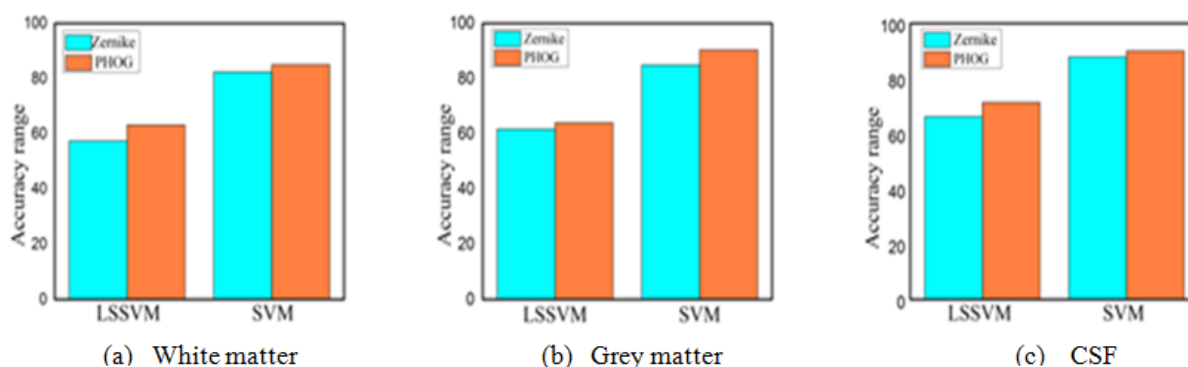


Fig. 6. Comparison of Zernike and PHOG features based on classifier accuracy for different brain tissues (a) White matter (b) Grey matter and (c) CSF

The considered groups and levels of extracted feature classification were carried out for each brain tissues. The classification measure accuracy is consider to evaluate the performance of LS-SVM and SVM. The average classification accuracy of ZM and PHOG feature for various brain tissues are shown in Fig. 6. It is observed that SVM gives more accuracy when compare to LS-SVM. It is notice that ZM give lesser accuracy and variation in brain tissues when compare to PHOG. This shows that PHOG that are extracted from WM, GM and CSF seems to have important discriminating features between normal, MCI and AD images.

TABLE II. CLASSIFICATION ACCURACY OF PHOG FEATURES USING LS-SVM AND SVM

PHOG (% Accuracy)	LS-SVM			SVM		
	WM	GM	CSF	WM	GM	CSF
LEVEL 3	94.8	98	97.6	98	99.2	98.8
LEVEL 2	94	96.4	95.6	96	97.6	96.8
LEVEL 1	58.4	60.4	70.4	60.8	74.4	74.4
Average	82.4	84.9	87.8	85	90.4	90

The classification result of PHOG features for each level is represent in Table 2. The results shows a that there exist a reliable tissue variation in every level in PHOG between the brain tissues. SVM perform better in each levels of PHOG than LS-SVM. In SVM it is observed that at each level there exist a difference in tissue variation in WM, GM and CSF. At each level GM appear to have high discrimination than WM and CSF. From the above result, it is clear that level 3 in SVM shows higher classification accuracy when compared to other levels. Hence SVM in level 3 gives maximum accuracy of 99.2% for grey matter than WM (98%) and CSF (98.8%). Thus the significant feature PHOG and its corresponding level is identified. The significant difference in GM is able to classify the normal, MCI and AD subjects. Another critical observation shows that changes in GM [26] cause shrinkage in hippocampus, cortical and sub-cortical along the discriminating directions. Such patterns of changes are well known to characterize the disease progression in AD and related dementia.

TABLE 3 COMPARISON OF ACCURACY OBTAINED BY THE PROPOSED METHODOLOGY AND CONVENTIONAL METHOD

Database	Approach	Accuracy	Reference
ADNI	SPM tissue segmentation + PCA+SVM	83.48%	27
ADNI	Fuzzy possibilistic tissue segmentation + SVM Classification	71%	28
ADNI	Proposed Method	90.4%	-

Table 3 compares the accuracy of the proposed method with other state of art methods. It shows that, the proposed framework gives improved accuracy than other methods. These findings suggest that these features can be a useful representation for characterizing brain tissue variations complementary to volumetric analysis for better diagnosis.

IV. CONCLUSION

In this work an attempt is made to analyse the tissue variation in normal, MCI and AD subjects from MR brain images. At the beginning delineation of non brain tissue was carried out using ROBEX tool. It is observed that it properly segment the non brain tissue using hybrid approach. Segmentation of a brain tissue from the skull stripped is carried out using multilevel Tsallis entropy. It is also identified from the results better segmentation is carried out based on the improved threshold values. The ZM and PHOG features are extracted for further evaluation. The significant feature set obtains using PCA. It is noticed that compare to ZM feature PHOG performs well. Results show that accuracy of SVM is higher than LS-SVM. Similarly in SVM, GM pattern variation is well diagnosed for normal, MCI and AD images using PHOG feature. These observation shows that GM shows a discriminate variation to classify normal, MCI and AD subjects effectively. These findings suggest that tissue variation can be a useful representation for characterizing dissimilarities in brain structure that is complementary to volumetric analysis. Thus, this framework could be used to study the neuropsychiatric disorder such as dementia. In future, this work could be extended by considering other regions such as caudate, hippocampus and thalamus from different views with more number of samples.

REFERENCES

- [1] Sarah Tomaszewski Farias, Dan Mungas, Bruce R. Reed, Danielle Harvey, and Charles DeCarli, MDet, "Progression of Mild Cognitive Impairment to Dementia in Clinics Community-Based Cohorts", *Archives of Neurology*, pp.1151-1157, Vol 66(9), 2009.
- [2] Nina B. Silverberg, Laurie M. Ryan and Maria C. Carrillo et al., "Assessment of cognition in early dementia", *Alzheimer's & dementia: the journal of the Alzheimer's Association*, pp.60-76, Vol7 (3), 2011.
- [3] <https://www.alz.co.uk/research/statistics>.
- [4] P. Kalavathi and V. B. Surya Prasath, "Methods on skull stripping of MRI head scan images-a review", *Journal of Digital Imaging*, Vol 29(3), pp.365-79, 2015.
- [5] Francisco J. Galdames, Fabrice Jaillet and Claudio A. Perez, "An Accurate Skull Stripping Method Based on Simplex Meshes and Histogram Analysis in Magnetic Resonance Images", *Rapport de recherche RR-LIRIS-2011-019*.
- [6] Juan Eugenio Iglesias, Cheng-Yi Liu, Paul Thompson and Zhuowen Tu, "Robust Brain Extraction across Datasets and Comparison with Publicly Available Methods", *IEEE Trans. on Medical Imaging*, 2011.
- [7] Lilia Lazli1, Mounir Boukadoum and Otmane Aït-Mohamed, "Brain Tissue Classification of Alzheimer Disease Using Partial Volume Possibilistic Modeling: Application to ADNI Phantom Images", 2017.
- [8] Sanjay Agrawal , Rutuparna Panda, Leena Samantaray and Ajith Abraham, "A novel automated absolute intensity difference based technique for optimal MR brain image thresholding", *Journal of King Saud University – Computer and Information Sciences*, 2017.

- [9] K. R. Anandh, C. M. Sujatha² and S. Ramakrishnan, “A Method to Differentiate Mild Cognitive Impairment and Alzheimer in MR Images using Eigen Value Descriptors”, *Journal of Medical System*, Vol 40 (1), pp.1-8, 2016.
- [10] Arora, S., Acharya, J., Verma, A., & Panigrahi, P. K., “Multilevel thresholding for image segmentation through a fast statistical recursive algorithm”, *Pattern Recognition Letters*, Vol. 29(2), pp. 119–125, 2008.
- [11] Qianqian Lin and Congjie Oun, “Tsallis entropy and the long-range correlation in image thresholding”, *Signal Processing*, Vol.92, pp.2931–2939, 2012.
- [12] Amir Tahmasbin, Fatemeh Saki and Shahriar B. Shokouhi, “Classification of benign and malignant masses based on Zernike moments”, *Computers in Biology and Medicine*, Vol 41(8), pp.726-35, 2011.
- [13] U. Rajendra Acharya, Yuki Hagiwarara, Joel E.W. Koha, Jen Hong Tana, Sulatha V. Bhandary, A. Krishna Rao and U. Raghavendra, “Automated screening tool for dry and wet age-related macular degeneration using pyramid of histogram of oriented gradients and nonlinear features”, *Journal of Computational Science*, Vol 20, pp.41-51, 2017.
- [14] G.Nagarajana, R.I.Minub, B Muthukumar, V.Vedanarayanan and S.D.Sundarsinghe, “Hybrid Genetic Algorithm for Medical Image Feature Extraction and selection”, *International Conference on Computational Modeling and Security*, Vol85, pp. 455-462, 2016.
- [15] Mahmoodi NM, Arabloo M and Abdi JLaccase, “Immobilized manganese ferrite nanoparticle: synthesis and LSSVM intelligent modeling of decolorization”, *Water Res*, Vol 67, pp. 216-226, 2014.
- [16] Takuya Inoue and Shigeo Abe, “Fuzzy support vector machines for multilabel classification”, *Pattern Recognition*, Vol 48(6), pp.2110–2117, 2015.
- [17] K.P. Baby Resma and Madhu S. Nair, “Multilevel Thresholding for Image Segmentation using Krill Herd Optimization Algorithm”, *Journal of King Saud University - Computer and Information Sciences*, 2018.
- [18] Liying Zheng and Kai Tian, “Detection of small objects in sidescan sonar images based on POHMT and Tsallis entropy”, *Signal Processing*, Vol. 142, pp.168–177, 2018.
- [19] Shanwen Zhang, Yihai Zhu, Zhuhong You and Xiaowei Wu, “Fusion of superpixel, expectation maximization and PHOG for recognizing cucumber diseases”, *Computers and Electronics in Agriculture*, Vol 140, pp. 338-347, 2017.
- [20] N. Dalal and B. Triggs, “Histograms of oriented gradients for human detection”, *Proc. of IEEE Conference on Computer Vision and Pattern Recognition*, pp. 886-893, 2005.
- [21] Christos Boutsidi, Michael W. Mahoney and Petros Drineas, “Unsupervised Feature Selection for Principal Components Analysis”, *Proceedings of the 14th International conference on Knowledge discovery and data mining*, pp.61-69, 2008.
- [22] Takuya Inoue and Shigeo Abe, “Fuzzy support vector machines for multilabel classification”, *Pattern Recognition*, Vol 48(6), pp.2110–2117, 2015.
- [23] Suykens JAK, Van, Gestel T, DeBrabanter J, DeMoor B, Vandewalle J Least squares support vector machines, *World Scientific Pub. Co., Singapore* (2002).
- [24] Mahmoodi NM, Arabloo M and Abdi JLaccase, “Immobilized manganese ferrite nanoparticle: synthesis and LSSVM intelligent modeling of decolorization”, *Water Res*, Vol 67, pp. 216-226, 2014.

- [25] Mehrdad Hesampour et al., “Nanofiltration of single and mixed salt solutions: Analysis of results using principal component analysis”, *Chemical Engineering Research and Design*, Vol 8, pp. 1569–1579, 2010.
- [26] Christiane Möller, Hugo Vrenken , Lize Jiskoot , Adriaan Versteeg, Frederik Barkhof, Philip Schelten and Wiesje M. van der Flier, “ Different patterns of gray matter atrophy in early- and late-onset Alzheimer’s disease”, *Neurobiology of Aging* , Vol 34(8), pp. 2014-22, 2013.
- [27] A. Domínguez , J. Ramírez , J. M. Górriz , F. Segovia , D. Salas-Gonzalez , F. J. Martínez-Murcia, I. A. Illán , “Statistical feature selection and classification models for Alzheimer’s disease progression assessment”, *IEEE Nuclear Science Symposium, Medical Imaging Conference and Room-Temperature Semiconductor Detector Workshop (NSS/MIC/RTSD)*, 2016.
- [28] Lilia Lazli ; Mounir Boukadoum ; Otmane Ait Mohamed, “Computer-Aided Diagnosis System for Alzheimer's Disease Using Fuzzy-Possibilistic Tissue Segmentation and SVM Classification”, *IEEE Life Sciences Conference (LSC)*, 2018.